Renewable and Sustainable Energy Reviews 21 (2013) 204–214

Contents lists available at SciVerse ScienceDirect

Renewable and Sustainable Energy Reviews

journal homepage: www.elsevier.com/locate/rser

Sustainable removal of non-condensable gases from geothermal waters

Anna Khaghani *, Abhijit Date, Aliakbar Akbarzadeh

Energy Conservation and Renewable Energy Group, School of Aerospace, Mechanical and Manufacturing Engineering, PO Box 71, Bundoora East Campus, RMIT University, Bundoora, Victoria 3083, Australia

ARTICLE INFO

Article history:
Received 31 August 2011
Received in revised form
3 December 2012
Accepted 9 December 2012
Available online 29 January 2013

Keywords:
Geothermal energy
Non-condensable gases
Eductor
Vacuum machine
Energy efficiency

ABSTRACT

Geothermal energy is becoming an attractive option for supplying the world with clean and sustainable energy. One of the highlighted issues in utilising the energy from geothermal systems is removal of non-condensable gases (NCGs) from geothermal waters. This paper discusses and reviews existing technologies for removing NCG with emphasis on their energy requirements further the possibility is investigated of using two-phase ejectors (also known as eductors) to remove NCGs from geothermal waters. Energy analysis of isothermal and adiabatic vacuum processes for removing non-condensable gases by an ideal vacuum machine are presented and later compared with the measured performance and with the energy consumption of commercial vacuum pumps and eductors. Advantages of removal of NCG using a passive method employing eductors and the prospect of improving the efficiency of these devices are also presented. Based on the experimental data, it is shown that eductors offer a sustainable alternative for NCGs removal from geothermal waters.

Contents

1. Introduction

Geothermal fluids contain non-condensable gases (NCGs) in various quantities. NCGs may have significant impact on the performance of power generation systems which use geothermal waters. In the situation where geothermal water is used as the working fluid in an expander for power generation [1], NCGs present in water can increase the pressure in the condenser and

* Corresponding author. Tel.: +61 395 695710.
E-mail addresses: anna.khaghani@student.rmit.edu.au (A. Khaghani), abhijit.date@rmit.edu.au (A. Date), aliakbar.akbarzadeh@rmit.edu.au (A. Akbarzadeh).

1364-0321/$ - see front matter Crown Copyright © 2012 Published by Elsevier Ltd. All rights reserved.
http://dx.doi.org/10.1016/j.rser.2012.12.001

Nomenclature

A	surface area (m^2)
D	diameter (m)
I	current (amp)
L	length [m]
m	mass (kg)
$\dot{m}$	mass flow rate (kg/s)
P	pressure (N/m^2)
$\dot{W}$	power (W)
R	specific gas constant (J/kg K)
SEC	specific energy consumption (J/kg)
t	time (s)
T	temperature (°C)
v	velocity (m/s)
V	voltage (Volts)
$\dot{V}$	volume flow rate (m^3/s)
w	specific energy (J/kg)
W	work (J)
x	distance (m)
ρ	density (kg/m^3)
α	eductor characteristic constant
γ	adiabatic index
η	efficiency

Subscripts

adia	adiabatic
atm	atmosphere
e	exit
f	final
i	initial
in	input
iso	isothermal
l	liquid
mf	motive fluid
r	relative
s	suction

therefore decrease the thermodynamic efficiency of the power generator.

Depending on the source, the fraction of the NCGs in geothermal water can vary from less than 0.2% by mass to greater than 12% by mass [2]. It is important that the selected NCG removal process is appropriate to the concentration of NCG in the source as the removal process uses a large amount of auxiliary power [3]. By using an appropriate NCG removal process the overall performance of the power plant can be improved [4].

The common NCGs present in geothermal water are a mixture of CO_2, H_2S, H_2, Hg, NH_3 and CH_4 [5]. The most prevalent gas is carbon dioxide constituting approximately 95% by weight of the mixture [3].

The following are some of the NCG removal methods used in industrial processes:

1. Extraction using commercially available vacuum pumps [6].
2. Steam ejectors used in order to create a vacuum which assists in the removal of NCGs [8].
3. Not allowing NCGs to enter the system: this can be achieved by degasification of the source fluid before it enters the system [9];
   a. Degasification by pressure reduction, as the quantity of a dissolved gas in a liquid is proportional to its partial pressure.
   b. Degasification by temperature increase. In some cases, however, the solvent and/or the solute decompose react with each other, or evaporate at high temperature and the rate of removal is less controllable.

Angulo et al. have been working on removal of NCG from flash geothermal steam. They have considered condensation and re-evaporation of the steam in a heat exchanger, upstream of a power plant [3]. The main component of their system was a vertical shell and tube heat exchanger with 50 titanium tubes. Steam was fed into the shell side of the heat exchanger. This flowed upwards and most of the steam condensed on the walls of the tubes. The non-condensable gases, together with a small amount of steam, were vented through a purge line located at the upper part of the shell. The condensate flowed into a transfer tank, which acted as a steam seal, and finally, into a storage tank, operated at a lower pressure than the shell side. In this way, a temperature difference was created between the incoming steam and the stored condensate. From the bottom of the storage tank, a pump transferred condensate to the flood box, from which it flowed inside the tubes. The latent heat of the incoming steam was transferred, causing a portion of the condensate to be evaporated, thus producing steam with a low gas content that was discharged at the upper part of the storage tank. The nominal capacity of their equipment was 0.4 t per hour of steam which resulted in achievement of a mean value of 94% for gas removal efficiency by their system. They also found that non-condensable gas removal efficiency was found to depend on the fraction of steam vented with the non-condensable gases [3].

Yildirim Ozcan and Gokcen have studied the net power output and specific steam consumption of a single-flash geothermal power plant which depended on the separator pressure, NCG fraction and wet bulb temperature of the environment. Three different conventional gas removal options were considered, which were a two-stage steam jet ejector system, a two-stage hybrid system and a two-stage compressor system. They found that increasing the NCG fraction decreases, by different amounts, the net power output for each option regardless of separator pressure. It was concluded that in relation to sensitivity of geothermal power plant performance to the NCG fraction, the compressor system is the most efficient and robust system where the influence of the NCG fraction is limited. On the other hand, steam jet ejectors are highly affected by increasing NCG fraction since the driving steam flow rate to the steam jet ejectors is directly related to NCG fraction [4].

Michaelides has investigated influence of non-condensable gases on turbine work, turbine efficiency and extraction work. For his study, as carbon dioxide constituted the major fraction of the non-condensable gases with its concentration always more than 85%, he assumed that the mass of non-condensable gases can be replaced by an equivalent mass-fraction of CO_2. Therefore, he assumed that an ideal gaseous mixture of CO_2 and steam enters the turbine. He concluded that the presence of non-condensable gases in geothermal steam power plants has an adverse effect on the net work produced. This is attributed both to the decrease of the turbine work and to the power supplied to the gas-extraction equipment. In his study, liquid brine is supplied to a primary flashing chamber where a small reduction of pressure releases most of the CO_2 and some steam. This mixture passes through an atmospheric turbine and is vented to the surroundings. The remaining brine, free of most of the CO_2, is

flashed and supplies a condensing turbine with steam containing a only small amount of CO_2. He showed that with a mass fraction of 0.2 of CO_2, 50% more work is needed compared to a conventional dual-flash system [5].

In this paper a liquid water ejector is investigated for achieving vacuum removal of NCGs as an alternative to using conventional vacuum pumps or steam ejectors. The main motivation for investigating a water ejector is that it is passive in operation (i.e. no moving parts) has low cost and is easy to maintain. As this type of vacuum device requires a continuous water flow, it could be used in a system which also uses water cooled condensers [10]. This would eliminate the need for additional pumps.

Ejectors are a very simple and practical solution to many pumping problems in various industries worldwide and typically their range of application is overlooked. They can be used alone or in multiple stages to create a range of vacuum conditions as well as being operated in transfer and mixing functions [11]. They are most commonly used to pump gases and vapours out of confined spaces in order to lower the pressure below ambient pressure. The simplicity and the passivity of these vacuum systems make the use of this device highly desirable in order to increase the viability of sustainable vacuum processes for removing NCGs.

There have been many studies on liquid-to-liquid ejectors and steam jet ejectors, but few on ejectors where the motive fluid is water and suction fluid is gas and which are usually termed eductors [11]. An experimental feasibility study on using eductors to remove NCGs has been done by Anna Khaghani et al. [12]. This paper further investigates the performance of commercially available eductors and compares it with that of commercial available vacuum pumps.

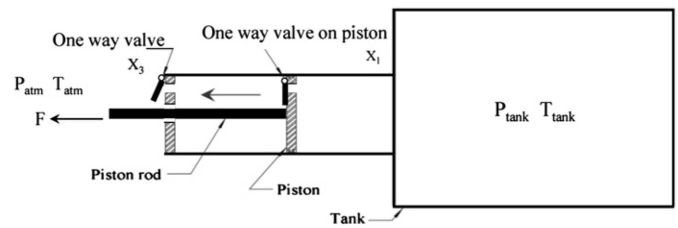


Fig. 1. Vacuum process.

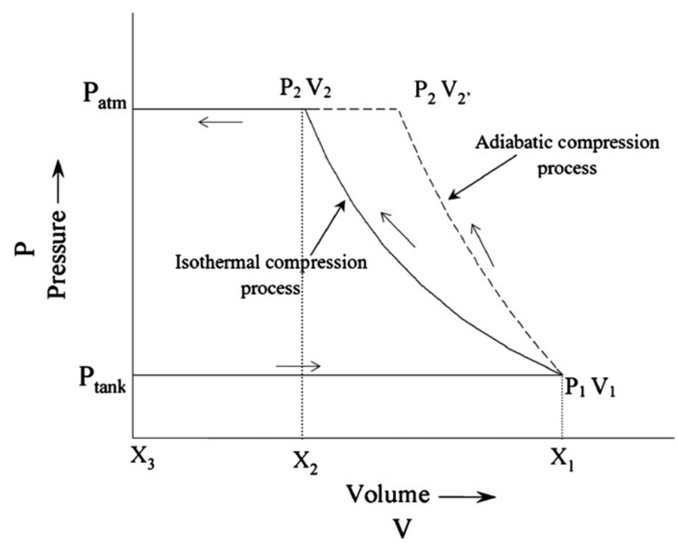


Fig. 2. *P–V* diagram for isothermal and adiabatic vacuum process.

2. Theoretical analysis and calculation of minimum energy required to remove and exhaust NCG

In this section attempts are made to calculate the theoretical minimum energy required to remove non-condensable gases from geothermal systems. Here the theoretical minimum specific energy consumption (J/kg) for this degassing process is calculated by considering the thermodynamic processes involved (adiabatic or isothermal), the pressure and temperature of the geothermal system and the atmospheric pressure to which the NCGs are exhausted. The required theoretical minimum specific energy consumption is subsequently used as a benchmark to compare available vacuum systems from the points of performance and sustainability.

Clearly the system with lowest specific energy consumption will be the most desirable in terms of environmental sustainability.

2.1. Ideal vacuum machine

The vacuum process can be idealised as increasing the pressure of the extracted gas from a lower pressure (P_{tank}) to atmospheric pressure (P_{atm}) by using a piston and cylinder device as shown in Fig. 1 [7].

If we consider the vacuum process as seen in the *P–V* diagram in Fig. 2, the work done to push 1 kg of air from the tank at a pressure of P_{tank} to atmospheric pressure, P_{atm}, can be calculated as below [8]

$$W_{1-2} = \int_{x_1}^{x_2} (p - p_{\tan k}) A\, dx = \int_{V_1}^{V_2} (p - p_{\tan k})\, dV \tag{1}$$

In which W_{1-2} is the work done to pull the piston from position X_1 to position X_2 and A is the area of the piston.

Assuming that the air is an ideal gas and that the process is isothermal [8]

$$PV = mRT = \text{constant} \tag{2}$$

The work done in this isothermal process can be written

$$W_{1-2} = \left(\int_{V_1}^{V_2} \frac{mRT_{\tan k}}{V} dV \right) - P_{\tan k}(V_2 - V_1) = mRT_{\tan k} \ln\left(\frac{V_2}{V_1}\right)$$
$$- P_{\tan k}(V_2 - V_1) = mRT_{\tan k} \ln\left(\frac{P_1}{P_2}\right) - P_{\tan k}\left(\frac{mRT_{\tan k}}{P_2} - \frac{mRT_{\tan k}}{p_1}\right)$$
$$= mRT_{\tan k}\left(\ln\left(\frac{P_1}{P_2}\right) - \frac{P_{\tan k}}{P_2} + \frac{P_{\tan k}}{p_1}\right) \tag{3}$$

By assuming $P_1 = P_{tank}$ and $P_2 = P_{atm}$, the work required becomes

$$W_{1-2} = mRT_{\tan k}\left(\ln\left(\frac{P_{\tan k}}{P_{atm}}\right) + 1 - \frac{P_{\tan k}}{P_{atm}}\right) \quad \text{(J)} \tag{4}$$

In addition, there will be extra work needed to push the compressed air out of the cylinder and into the atmosphere. For an isothermal process, this is shown as W_{2-3}

$$W_{2-3} = mRT_{\tan k}\left(\frac{P_{\tan k}}{P_{atm}} - 1\right) \quad \text{(J)} \tag{5}$$

By combining Eqs. (4) and (5) the total work done in the process becomes

$$W_{iso} = mRT_{\tan k} \ln\left(\frac{P_{\tan k}}{P_{atm}}\right) \quad \text{(J)} \tag{6}$$

Therefore, the specific work needed to extract unit mass of air from tank pressure (P_{tank}) and deliver it to the atmospheric in an

isothermal process can be calculated as

$$w_{iso} = \frac{W_{iso}}{m} = RT_{\tan k} \ln\left(\frac{P_{\tan k}}{P_{atm}}\right) \quad (\text{J/kg}) \tag{7}$$

The change of the specific work with respect to the tank pressure (P_{tank}) can be written as

$$\frac{dw_{iso}}{dP_{\tan k}} = RT_{\tan k}\left(\frac{1}{P_{\tan k}}\right) \tag{8}$$

A similar derivation can be made for the case of adiabatic compression. However, as shown in Fig. 2 the isothermal process offers a lower work requirement for extracting unit mass of air from a tank and raising its pressure in order to deliver it to the atmospheric.

Accordingly, Eq. (7) is used to calculate the minimum energy required in the vacuum process and it is also used to calculate the efficiency of the vacuum devices considered in this research, including eductors and vacuum pumps.

To complete the picture the thermodynamics of an adiabatic process instead of isothermal can be also considered as [8]

$$PV^{\gamma} = \text{constant} \tag{9}$$

Considering this process, the work needed to change the pressure of 1 kg of NCG from P_{tank} to P_{atm} can be calculated as

$$w_{adia} = RT_{atm}\left[\frac{(P_{atm}/P_{\tan k})^{1-1/\gamma} - \gamma}{1-\gamma} - \left(\frac{P_{atm}}{P_{\tan k}}\right)\left(\frac{P_{\tan k}}{P_{atm}}\right)^{1/\gamma}\right] \quad (\text{J/kg}) \tag{10}$$

As represented schematically in Fig. 2, the adiabatic process of gas removal would require more work. The required theoretical power for these processes is

$$Power = w_{iso/adia}\frac{dm}{dt} \tag{11}$$

The theoretical power required for gas removal can be calculated by multiplying the desired mass flow rate of the gas [$\dot{m}$, (kg/s)] and the specific energy given by Eq. (7)

$$\dot{W}_{\min imum} = \dot{m} \times w_{iso} \tag{12}$$

Eq. (12) represents the minimum power required for the vacuum process.

As will be shown later, in practice, the energies consumed by eductors and by vacuum pumps are substantially greater. One of the main purposes of the present paper is to compare the efficiencies of eductors and vacuum pumps in removing NCGs from geothermal waters against a benchmark of the theoretical power calculated in Eq. (12).

For this purpose, the efficiency of the actual vacuum process can be defined

$$\eta_{actual} = \frac{electric\ power}{\dot{m} \times w_{iso}} \tag{13}$$

In Eq. (13), the numerator (electric power) is the electrical power consumed by the motor in the case of a vacuum pump ($I \times V$) or the electrical power required by the motor driven pump used to creating the pressure difference in the case of an eductor (see Section 2.2).

The power required by a conventional vacuum machine is usually provided in the supplier's specifications and can also be calculated by multiplying the measured values of electrical current and voltage. For the case of an educator, the pump power can be defined as

$$Pump\ power = \frac{\dot{V}\Delta P}{\eta_{pump} \times \eta_{motor}} \tag{14}$$

In Eq. (14), $\dot{V}$ is the volume flow rate of water in m^3/s as a primary fluid and ΔP is the pressure difference across the eductor in Pa. Also η_{pump} refers to the mechanical efficiency of the pump and η_{motor} corresponds to the electrical efficiency of the pump motor. These efficiencies are in the order of 60% and 80%, respectively. In the present analysis, a combined efficiency of 50% is considered for the water pump (i.e. motor and pump combined).

2.2. Ejectors

A single-stage ejector (sometimes also known as an eductor or jet pump) in its most basic form contains an actuating nozzle, suction chamber and a diffuser as shown in Fig. 3. The primary fluid (which can be liquid, vapour or another gas) flows through a tube which converges to a driving nozzle making the fluid accelerate and decrease in pressure due to the venturi effect [13]. Upon exiting the driving nozzle, the fluid is at a high velocity and a very low pressure and it entrains the stagnant secondary fluid into its flow within the suction chamber.

The mixture of primary and secondary fluids is then accelerated into the converging section of the ejector due to the rapid increase in velocity as the pressure decreases. As the mixture travels through the diffuser its pressure rises as the cross-sectional area increases and the velocity consequently decreases [14].

The basic concept for an eductor involves taking a high-pressure motive fluid and accelerating it through a tapered nozzle. This fluid then enters a secondary chamber where friction force between the molecules of it and a secondary fluid (gas) causes this secondary fluid to be entrained. These fluids are intimately mixed together and discharged from the eductor [15].

As P_1, P_s and v_1 are known for a specific situation; the velocity of fluid exiting the active nozzle v_2 can be calculated using the Bernoulli equation:

$$\frac{P_1}{\rho_l} + \frac{v_1^2}{2} = \frac{P_s}{\rho_l} + \frac{v_2^2}{2} \tag{15}$$

also

$$v_2 = \frac{\dot{V}}{A_2} \tag{16}$$

$$v_1 = \frac{\dot{V}}{A_1} \tag{17}$$

Using the above equations, Eq. (15) can be written as

$$P_1 - P_s = \frac{\rho_l \dot{V}_l^{\,2}}{2A_2^{\,2}}\left(1 - \frac{D_2^{\,4}}{D_1^{\,4}}\right) \tag{18}$$

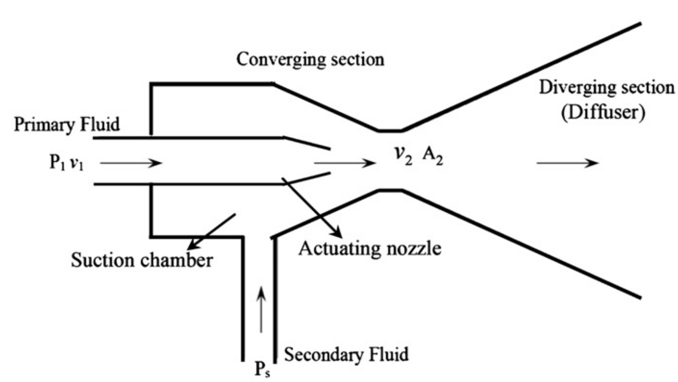


Fig. 3. Schematic of ejector.

where D_1 and D_2 are the inlet diameter of eductor and exit diameter of the nozzle, respectively, and A_1 and A_2 are the corresponding cross-sectional areas.

Knowing the geometric parameters D_1 and D_2, Eq. (18) provides a basis from which the minimum suction pressure (P_s) can be calculated for any given upstream pressure and volumetric flow rate of the primary fluid.

The power consumed by the eductor can be calculated by knowing the pressure of the primary fluid (upstream), its volumetric flow rate, and the pressure of the atmosphere into which the air water mixture is exhausted

$$Power = \dot{V} \times \Delta P = \dot{V} \times (P_1 - P_{atm}) \quad (19)$$

The pumping power needed to run an eductor and its efficiency can be determined experimentally by measuring parameters including the volumetric flow rate of the primary fluid and the inlet and the discharge pressures.

Assuming values for the mechanical efficiency of the pump and the electrical efficiency of the pump motor, the electrical power consumed to create the suction effect may be calculated from Eq. (14).

2.3. Commercially available vacuum pump

The operating process for a commercially available vacuum pump is shown in Fig. 4, where the vacuum pump consumes electrical power in order to exhaust the air from the tank and deliver it at atmospheric pressure.

The electrical input power is calculated by

$$Power_{in} = VI \quad (20)$$

The mass flow rate of the air can be calculated using the measured volumetric air flow rate at the outlet using the following equation:

$$\dot{m}_{air} = \frac{\dot{V}_{air} P_{atm}}{R T_{atm}} \quad (kg/s) \quad (21)$$

The specific energy consumption (SEC) is therefore calculated as

$$\text{Specific energy consumption} = \frac{power_{in}}{\dot{m}_{air}} \quad (22)$$

3. Experimental analysis

3.1. Comparison of the measured performance of commercial vacuum pumps with that of an ideal vacuum machine

In this section, attempts are made to determine the efficiency of the commercially available vacuum machines. In order to do this, the specific electric power consumed by the machine to achieve a certain level of vacuum is compared with that of an ideal vacuum system.

The power of a commercially available vacuum pump was measured as illustrated in Fig. 5. The inlet pressure of the air was controlled by a pressure control valve to assess the performance of the vacuum pump at different pressures. A vacuum gauge with uncertainty of $\pm 1\%$ was used for measuring the pressure in the range of 0–100 kPa. The atmospheric pressure in the laboratory was measured using a standard barometer. The absolute pressure was then calculated from

$$P = P_{atm} + P_{gauge} \quad (23)$$

The current and voltage were recorded in order to determine input power for each stage using a voltmeter with uncertainty of $\pm 1.5\%$ and an ammeter with uncertainty of $\pm 2.5\%$. Although its influence was minor, adjustments were made to take into account the power factor. The volume flow rate of the extracted air was measured by using a TSI 4000 series flow meter with uncertainty of $\pm 2\%$ which was designed for a variety of gas flow measurement applications in the range of 0–300 l/min.

The arrangement of the experiment is shown in Fig. 6. This experiment was conducted for both increasing and decreasing ranges of openings of the pressure regulating valve (fully open to fully close) providing corresponding vacuum pressures from atmospheric pressure to the minimum achievable vacuum pressure and back to atmospheric pressure. For each operating condition, current (I), voltage (V), pressure at the inlet and outlet of the vacuum pump (Pa), the flow rate of air (l/min) and atmospheric pressure (Pa) were recorded for use in performance analysis.

The recorded experimental data for two of the tests are shown in Table 1.

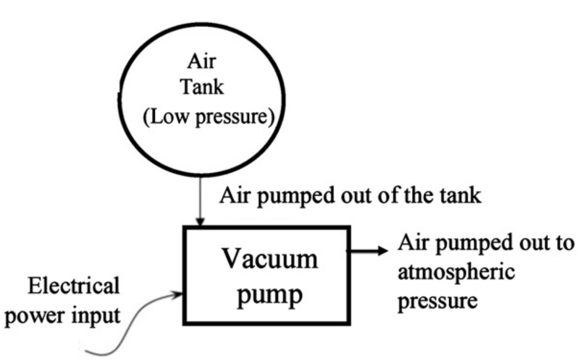


Fig. 4. Schematic of a vacuum pump.

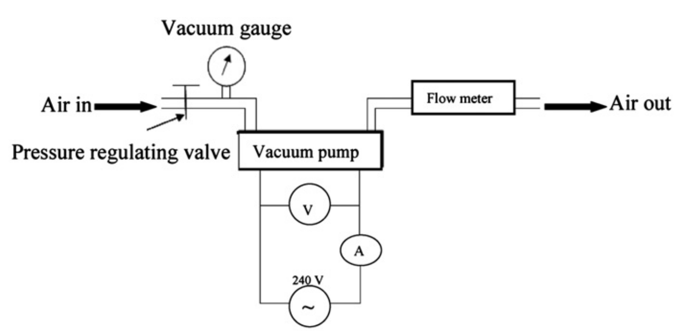


Fig. 5. Schematic set up for the vacuum pump.

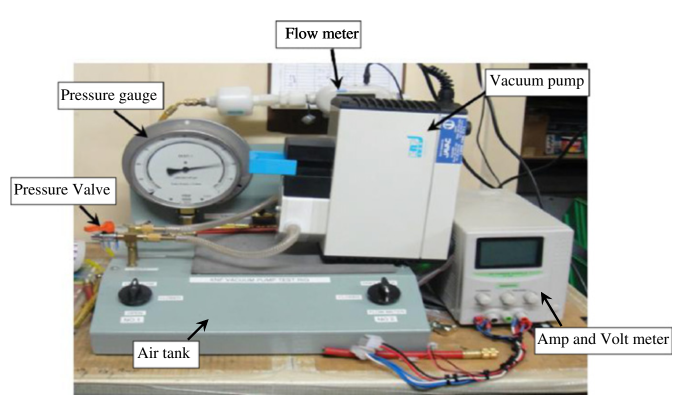


Fig. 6. Experimental set-up for vacuum pump performance analysis.

Table 1
Experimental data for commercially available vacuum pump for two tests.

Test 1 (atm to min vacuum pressure)						Test 2 (min vacuum to atmospheric pressure)					
P_{atm} (kPa)	T_{tank} (°C)	P_{tank} (kPa)	$\dot{V}$ (l/min)	V (volts)	I (Amps)	P_{atm} (kPa)	T_{tank} (°C)	P_{tank} (kPa)	$\dot{V}$ (l/min)	V (volts)	I (Amps)
100	16	100	22	248.5	1.2	100	17.4	10	0.75	248.5	1.2
100	16	90	18.5	248.5	1.2	100	16.9	20	2.45	248.5	1.2
100	16	80	15.7	248.5	1.2	100	16.6	30	4.35	248.5	1.2
100	16.2	70	13.5	248.5	1.2	100	16.5	40	6.42	248.5	1.2
100	16.2	60	11.03	248.5	1.2	100	16.4	50	8.80	248.5	1.2
100	16.3	50	8.74	248.5	1.2	100	16.4	60	11.15	248.5	1.2
100	16.5	40	6.3	248.5	1.2	100	16.3	70	13.31	248.5	1.2
100	16.8	30	4.25	248.5	1.2	100	16.3	80	15.45	248.5	1.2
100	17	20	2.45	248.5	1.2	100	16.1	90	17.68	248.5	1.2
100	17	10	0.68	248.5	1.2	100	16	100	21.6	248.5	1.2

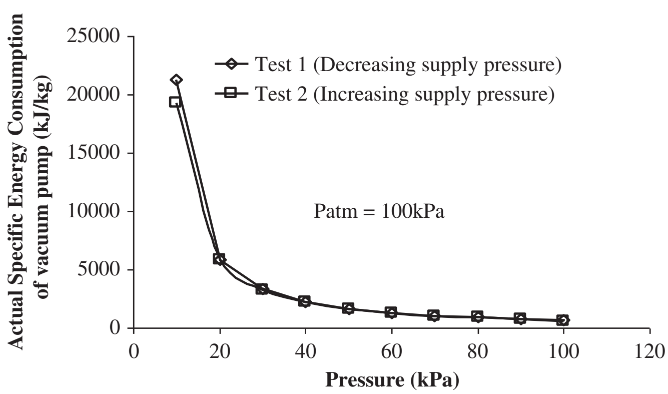


Fig. 7. Experimental specific energy consumption for two tests on a commercial vacuum pump as a function of supply air.

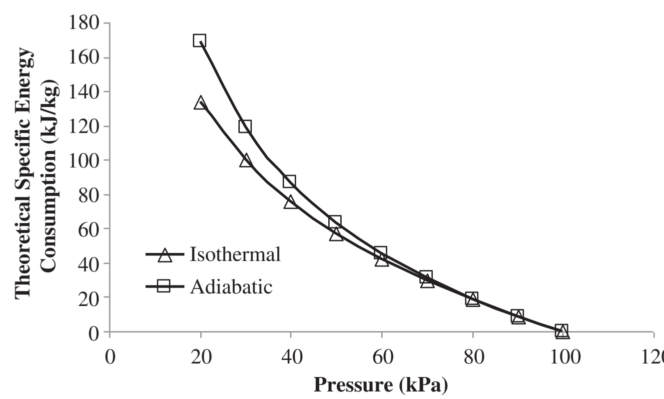


Fig. 8. Comparison of theoretical specific energy consumption for isothermal and adiabatic vacuum process.

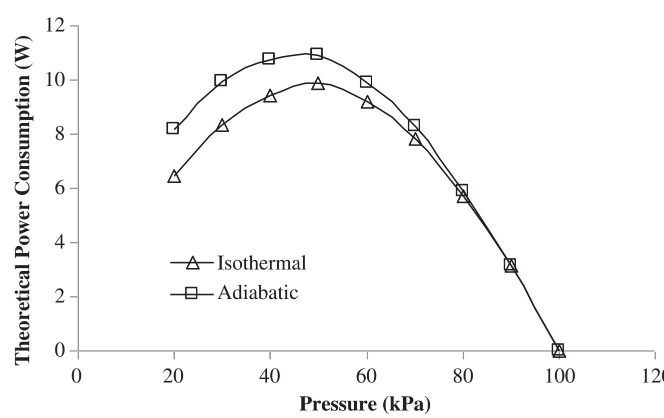


Fig. 9. Comparison of theoretical power for isothermal and adiabatic vacuum process of an ideal vacuum machin with the capacity of the vacuum pump under consideration.

Specific energy consumption of the vacuum pump at each air supply pressure was calculated from

$$SEC_{vacuum\ machin} = \frac{electrical\ power\ consumed\ by\ the\ machine}{\dot{m}_{air}} \tag{24}$$

The results are shown in Fig. 7.

This is the preferred parameter for comparison of theoretical and measured data. The graph in Fig. 7 shows close agreement between the results obtained during a reducing pressure test (Test 1) and an increasing pressure test (Test 2). It can be seen that the specific energy consumption for the vacuum pump increases as the inlet pressure is reduced.

3.2. Comparison of performance of a vacuum pump with an ideal vacuum machine

Based on the manufacturer's data sheets for the vacuum pump, which relate the flow rate of the entrained air to the suction pressure, theoretical analysis has been performed by assuming the vacuum pump to be ideal. The theoretical work and power for the isothermal and adiabatic processes are calculated by using Eqs. (7), (11) and (10), respectively.

The graphs of theoretical specific work and theoretical power for the isothermal and adiabatic processes for a commercial vacuum pump are shown in Figs. 8 and 9, respectively, and these figures can be compared to the measured values.

By using Eq. (24), the theoretical-specific energy consumption was calculated and is plotted in Fig. 8.

It is evident that the adiabatic work is greater than the isothermal work and both increase with decreasing inlet pressure. This is because work in adiabatic vacuum processes is higher than that in isothermal processes. Practical processes lie somewhere between the isothermal and adiabatic processes.

It can be seen that by decreasing the pressure, the theoretical power initially increases before decreasing.

Fig. 10 shows the specific energy consumption from an experimental test on a vacuum pump and compares it with the theoretical analysis for both adiabatic and isothermal processes as calculated from Eq. (7).

It can be concluded that at high pressure, the theoretical- and experimental-specific energy consumptions become closer. However, as the pressure is decreased, the experimental energy consumption rises up dramatically, because of the reduced mass flow rate of air, whereas the energy consumption of the vacuum pump has much less variation.

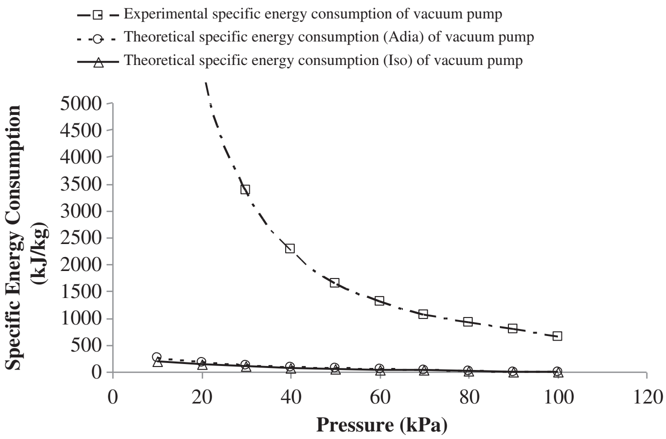


Fig. 10. Comparison of experimental and theoretical specific energy consumption for vacuum pump.

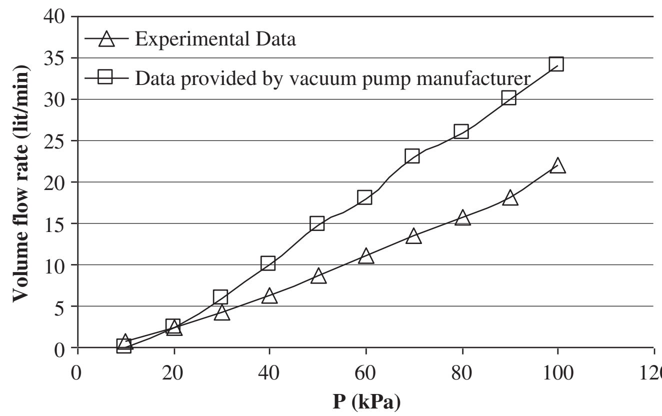


Fig. 12. Comparison of experimental and supplied data for a commercially available vacuum pump.

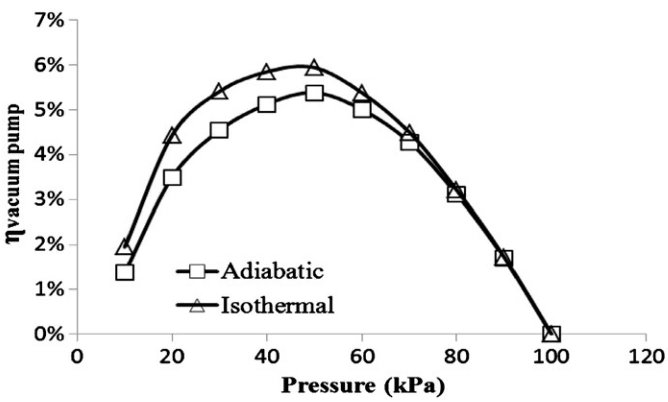


Fig. 11. Relative efficiency of a commercial vacuum pump.

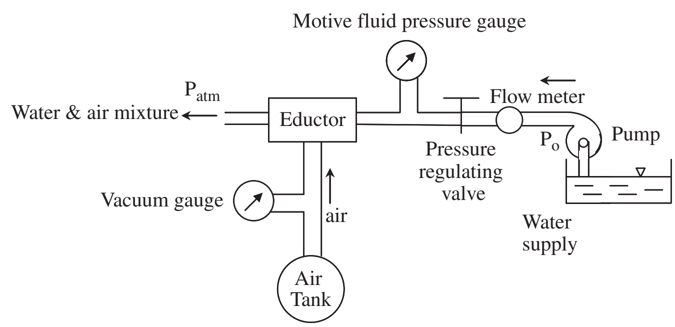


Fig. 13. Schematic of the experimental set-up for the eductor.

Relating the SEC by theoretical analysis to that from experimental data as shown in Fig. 10, the efficiency of the vacuum pump may be expressed as

$$\eta_{vacuum\,pump} = \frac{theoretical\quad SEC}{experimental\quad SEC} \tag{25}$$

Fig. 11 shows the efficiency of a commercial vacuum pump by considering the vacuum process as an isothermal process or as an adiabatic process.

For a vacuum pump, the energy consumption is close to constant because of the characteristics of the pump motor. An ideal vacuum machine will consume very little energy at atmospheric pressure at the inlet even though pumping a large amount of air. From Fig. 11, it can be seen that the efficiency of the typical vacuum pump tested was maximum at 50 kPa and achieved a value of 5.8%.

Fig. 12 compares the measured data with the data provided by a commercial vacuum pump manufacturer.

3.3. Comparison of theoretical and measured results for a commercially available water–gas ejector (eductor)

Here the results from a series of tests on two commercially available eductors are presented. The main purpose of the tests was to determine the specific energy consumption of an eductor at different suction pressures and to compare the results with the performance of a commercially available vacuum pump as presented in Fig. 11. Furthermore the performance of eductors is assessed against that of an ideal vacuum machine and conclusions have been drawn concerning the efficiency of an eductor as a possible sustainable candidate for removal of non-condensable gases from geothermal water.

In order to gain better understanding of eductor design and to establish the influence of different geometric parameters of an eductor on its efficiency, several performance tests on available eductors were conducted.

Testing an off the shelf eductor was initially planned in order to validate the theory of the base calculations on which the rest of the project will be later built. The suction ability of the nozzle was to be determined and a realistic potential volume of displaced air to be identified. The vacuum ability of a single phase ejector was investigated experimentally in order to find out whether or not it would be sufficient to evacuate and sustain the low pressure required.

A schematic of the eductor test rig is shown in Fig. 13. The test facility consisted of a water supply reservoir, a water pump, a flow meter, a pressure regulating valve, a pressure gauge, an eductor, a vacuum gauge and an air tank. The ejector is water driven and in the converging section, pressure drop occurs. The air from the tank, as the secondary fluid, is entrained by the water jet. In the diverging section, the mixture pressure increases and it is vented to atmosphere.

In this experiment, a 20 l tank equipped with a vacuum gauge was used. The 550 W water pump could produce a head of 600 kPa pressure and could deliver 55 l/min of water. The flow rate of the system was measured by a flow meter with the accuracy of 0.1%. Also, by using a bucket and stop watch method for measuring the flow rate of the water at the outlet, the accuracy of the flow meter was assessed. The supply water pressure to the eductor was measured using a pressure gauge (0–500 kPa) with uncertainty of $\pm 1\%$.

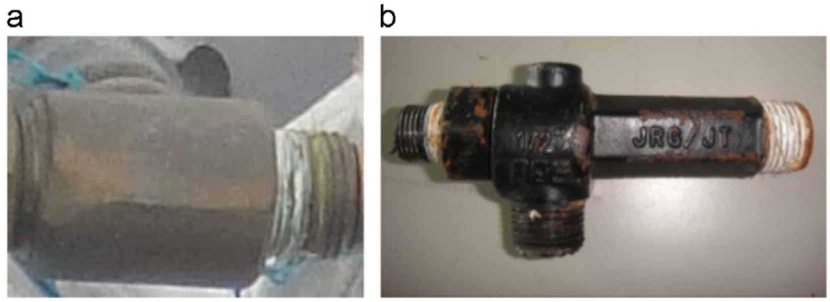


Fig. 14. The two eductors used in the experiments: (a) eductor 1 and (b) eductor 2.

Table 2
Experimental data for eductor at two different motive fluid pressures.

P_{mf}=300 kPa					P_{mf}=200 kPa				
P_{atm} (kPa)	T_{tank} (°C)	P_{tank} (kPa)	Time (s)	$\dot{V}$ (l/min)	P_{atm} (kPa)	T_{tank} (°C)	P_{tank} (kPa)	Time (s)	$\dot{V}$ (l/min)
100	16.2	100	0	0	100	16.5	100	0	0
100	16.2	91	6.54	0.22	100	16.5	91	5.78	0.163
100	16.2	86	15.46	0.22	100	16.5	81	16.57	0.163
100	16.2	81	17.52	0.22	100	16.6	71	32.98	0.163
100	16.3	71	29.72	0.22	100	16.6	61	58.63	0.163
100	16.4	66	37.22	0.22	100	16.6	56	74.92	0.163
100	16.4	61	45.66	0.22	100	16.6	51	93.34	0.163
100	16.5	56	55.88	0.22	100	16.6	46	114.25	0.163
100	16.5	51	68.06	0.22	100	16.6	41	140.33	0.163
100	16.5	46	81.91	0.22	100	16.6	36	170.49	0.163
100	16.7	41	98.28	0.22	100	16.7	31	202.25	0.163
100	17	36	117.29	0.22	100	16.7	26	241.12	0.163
100	17	31	140.09	0.22	100	16.7	21	290.15	0.163
100	17	26	167.80	0.22	100	17	16	369.10	0.163
100	17	21	202.71	0.22	100	17	11	499.57	0.163
100	17	16	249.07	0.22	100	17	8	1079.03	0.163
100	17.3	11	315.84	0.22	100	17.1	6	1800.00	0.163
100	17.3	6	460.77	0.22					
100	17.5	5	514.27	0.22					
100	17.5	4	603.47	0.22					
100	17.5	3	703.12	0.22					
100	17.6	2.5	900	0.22					

In this experiment, two eductors were used. The first ejector (here we call it eductor 1) was originally used to create a vacuum using steam as the primary fluid, but was driven by water flow in the current tests. The second ejector (here we call it eductor 2) was a commercially produced device to create vacuum using liquid water as the motive fluid. In Fig. 14, both ejectors are shown.

The test procedure started with the air tank pressure equal to the atmospheric pressure and at this stage the pump was started and the flow of water through the eductor caused the pressure in the tank to be decreased. Data were gathered on the water flow rate, pressure of the primary fluid as it entered the eductor measured by the pressure gauge, as well as tank pressure as functions of time. This process continued until there was no further reduction in the tank pressure. At this stage, the setting of the pressure regulating valve as shown in Fig. 13 was changed and then the above process of data collection was repeated.

3.4. *Test results*

Table 2 shows the experimental data during the tests on the eductors at different motive fluid pressures.

In Fig. 15, test results for the two eductors 1 and 2 for the maximum motive fluid pressure are shown. In this figure, the drop of the tank pressure is presented as a function of time for the two eductors 1 and 2.

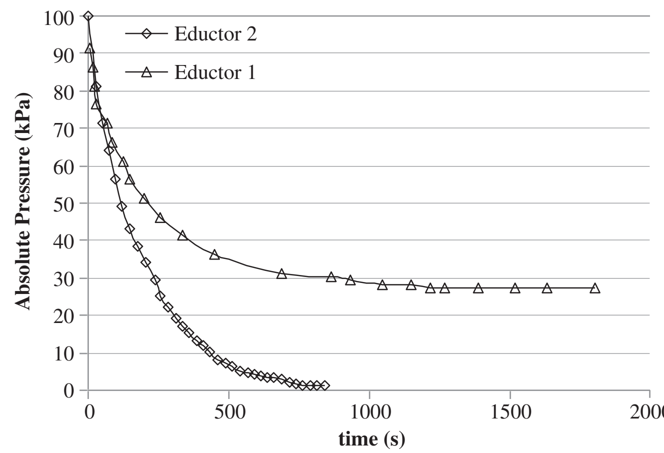


Fig. 15. Vacuum ability of two ejectors.

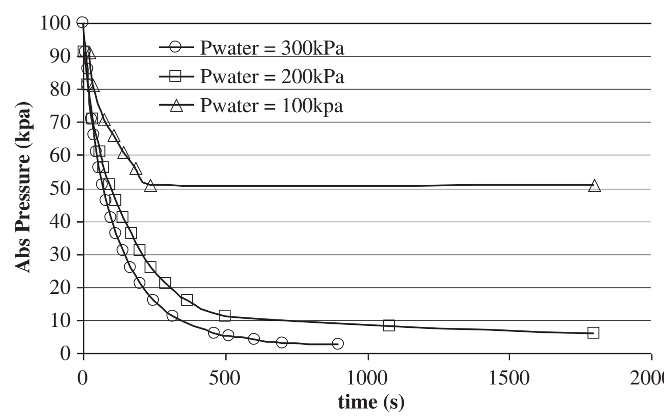


Fig. 16. Pressure drop in the tank using eductor 2 for different primary fluid pressures.

It can be seen that eductor 1 which was originally designed and limited to use steam as its primary fluid cannot reduce the tank pressure to the required low level. In this case, the eductor has been able to reduce the pressure of the tank to only 27 kPa. However, eductor 2 which was originally been used to use water as primary fluid has achieved very low pressure (almost 2 kPa) in the tank in less time.

Test results are shown in Fig. 16 for eductor 2 for different primary fluid pressures. In this figure, the drop of the tank pressure is shown as a function of time.

3.4.1. *Estimating the specific energy consumption of the eductors*

Energy is required to produce the suction effect of an eductor and the amount of energy consumed for unit of mass of air will be

a good measure of viability of the proposed system for degassing geothermal water. In order to calculate the specific energy consumption of this device for various motive fluid pressures and different ambient pressures, it is necessary to know the mass flow rate of air ($\dot{m}_{air}$). However, direct measurement of mass flow rate of air was very difficult, so an indirect method to estimate the mass flow rate of air out of the tank was used. Following are the equations used for indirect estimation of mass flow rate.

For an ideal gas, we have

$$P_{\tan k}V_{\tan k} = m_{\tan k}RT_{\tan k} \tag{26}$$

From Eq. (26)

$$m_{\tan k} = \frac{P_{\tan k}V_{\tan k}}{RT_{\tan k}} \tag{27}$$

By differentiating Eq. (27)

$$\frac{dm_{\tan k}}{dt} = \frac{V_{\tan k}}{RT_{\tan k}}\cdot\frac{dP_{\tan k}}{dt} \tag{28}$$

The mass flow rate of air ($\dot{m}_{air}$) out of the air tank and into the eductor is related to $m_{\tan k}$ and time as follows:

$$\dot{m}_{air} = -\frac{dm_{\tan k}}{dt} \tag{29}$$

By combining Eqs. (28) and (29)

$$\dot{m}_{air} = -\frac{V_{\tan k}}{RT_{\tan k}}\cdot\frac{dP_{\tan k}}{dt} \tag{30}$$

Using Eq. (30), knowing the volume of the tank, the tank temperature and using data available from Fig. 16 the mass flow rate of the air ($\dot{m}_{air}$) can be estimated. Evidently dP_{tank}/dt is not readily available from Fig. 16 and it must be approximated by using the data in Fig. 16. However, considering the exponential decay of the pressure in the air tank, it was thought better to perform curve fitting using an exponential function and using the resulting equations to approximate the variation of tank pressure with time.

Considering the data in Fig. 16, it has been concluded that the variation of P_{tank} with time is best presented by the following function:

$$P_{\tan k} = f(t) = P_f + (P_o - P_f)e^{-\alpha t} \tag{31}$$

In Eq. (31), P_f is the lowest pressure achieved in the tank and P_o is the initial tank pressure which is same as atmospheric pressure. Also, α is a parameter which needs to be determined.

Therefore, to find the best corresponding curve, α must be found by minimising the value of parameter D defined below

$$D = \sum_{i=1}^{n}[f(t_i) - P_i]^2 = \sum_{i=1}^{n}[P_f + (P_o - P_f)e^{-\alpha t} - P_i]^2 \tag{32}$$

By minimising the value of Eq. (32), α can be calculated for different pressures of motive fluid. This was done by varying α, examining the values of D and looking for its minimum.

The results of the curve fitting exercise are shown in Fig. 17, where the actual data and the curves of best fit are presented for three different upstream pressures of the eductor.

Fig. 17 indicates reasonable agreement between the curves obtained from the derived equation for pressure drop for different motive fluid pressures and those from the actual data.

The value of dP_{tank}/dt can be calculated by taking the derivative of Eq. (31) as below

$$\frac{dP_{\tan k}}{dt} = P_f\alpha e^{-\alpha t} \tag{33}$$

From Eq. (33), the value of dP_{tank}/dt is calculated for each motive fluid pressure at any time using the corresponding value of α. Mass flow rate of the air ($\dot{m}_{air}$) is calculated using Eq. (30).

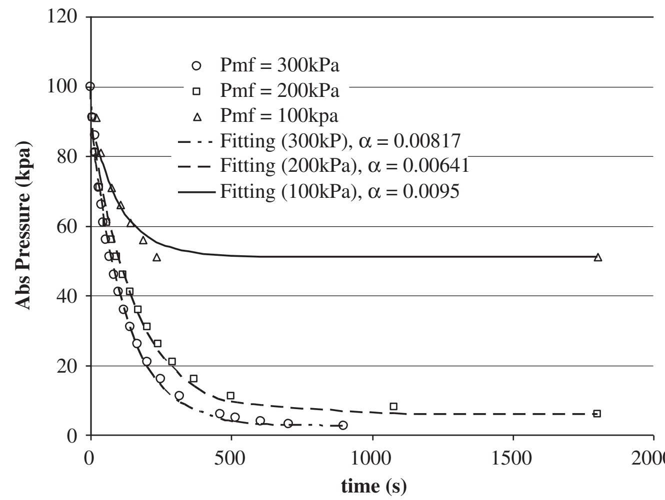


Fig. 17. Fitting curves for pressure drop in second ejector in different motive fluid pressures.

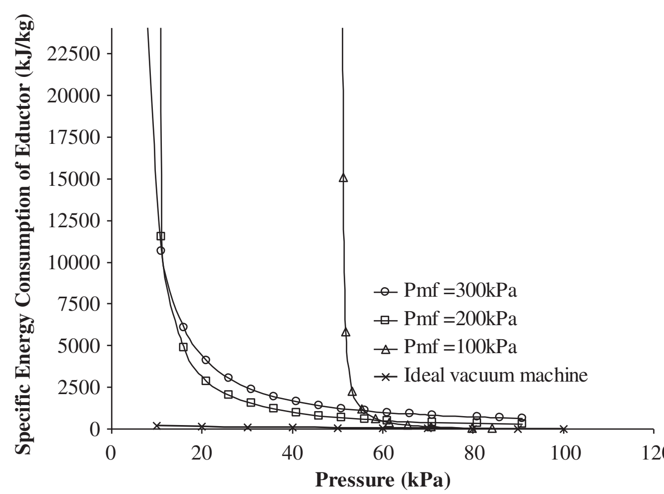


Fig. 18. Experimental and theoretical specific energy consumption for eductor in different motive fluid pressures.

The specific energy consumption of the eductor ($SEC_{eductor}$) is calculated from Eqs. (14) and (22).

In Fig. 18, the $SEC_{eductor}$ is shown for three different motive fluid pressures. On the same figure, the SEC of an ideal vacuum machine is also shown.

As it can be seen from Fig. 18, when the pressure of the tank decreases the specific energy consumption increases noticeably for eductors. In addition, decrease in motive fluid pressure has a direct effect of increasing the specific energy consumption of the eductor. It can also be seen that at high tank pressure and lower vacuum levels, the theoretical-specific energy consumption is close to experimental results for the eductor. However, as the pressure of the tank is reduced, the discrepancy increases. This is because of the small amount of the air which remains in the tank at low pressure.

The efficiency of the eductor at any point can be calculated using Eq. (13). Fig. 19 shows the efficiency curves of the second eductor estimated using experimental results combined with Eq. (15). In Eq. (18), the pumping power is estimated using the measured mass flow rate of water and the pressure drop across the eductor and considering an overall efficiency of 0.5 for water pump.

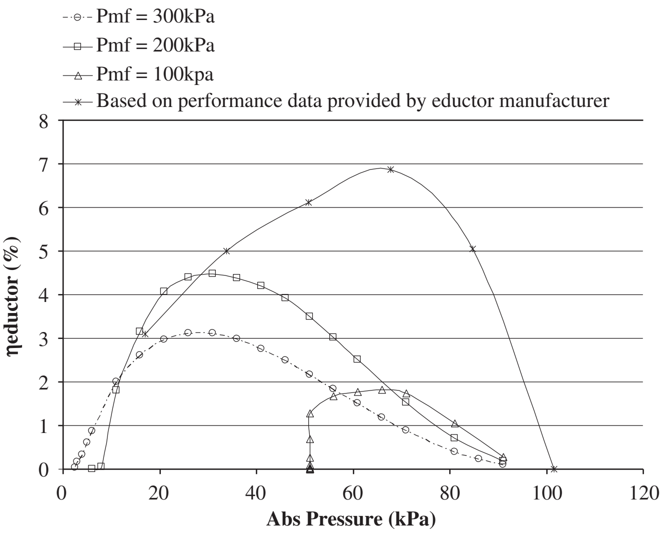


Fig. 19. Efficiency of the eductor for different motive fluid pressures.

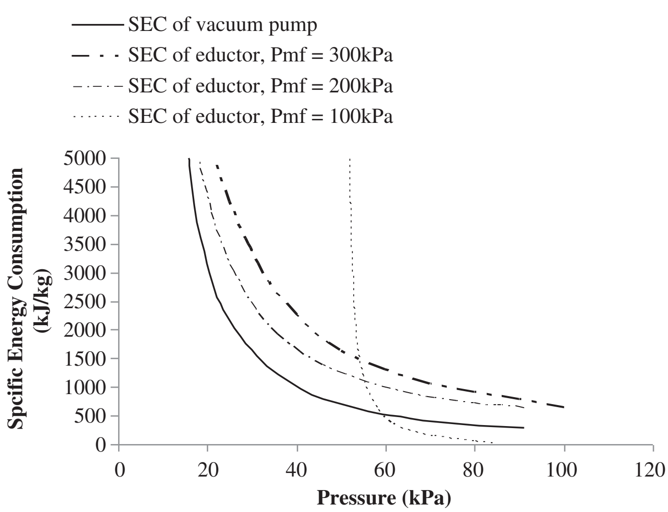


Fig. 20. Comparison of specific energy consumption for eductor performing in different motive fluid pressures and the commercial vacuum pump.

It can be deduced from Fig. 19 that the eductor has a maximum efficiency at a particular motive fluid pressure which in this case is 200 kPa. In the same figure, the efficiency of the eductor is presented using the data available from the manufacturer.

3.5. Comparison of performance of the vacuum pump and the eductor

In order to make sensible comparison of the performances of the vacuum pump and eductor, Fig. 20 shows the specific energy consumption of the vacuum pump and eductor at three different motive fluid pressures.

In addition the efficiency curves of the vacuum pump and the second eductor are shown in Fig. 21 using experimental results and Eq. (15). The error analysis show 1.03% uncertainty for the efficiency of the vacuum pump and 1.65% uncertainty for the efficiency of the eductor. It can also be seen that at pressures below 20 kPa (abs) the ejector has higher efficiency then a commercially available mechanical vacuum pump.

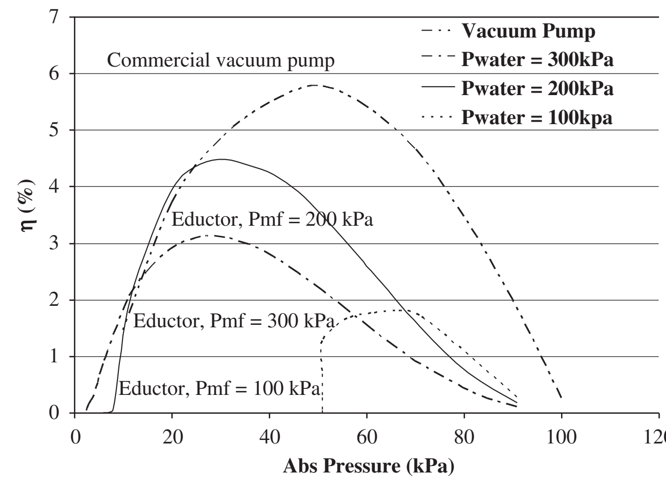


Fig. 21. Comparison of efficiencies for the commercial vacuum pump and the eductor for different motive fluid pressures.

4. Discussion of results

Theoretical and experimental results for SEC show close agreement at high tank pressure for both vacuum pump and eductor. However, at low pressure the disparity between the theoretical and experimental results increases. This is attributed to the smaller amount of air left in the tank as the tank pressure decreases while the vacuum ability of these devices remains constant during the whole process. Therefore, for the geothermal applications in which running water is available[1], eductors can be installed to remove non-condensable gases. This will have a significant effect on reducing the parasitic losses by removing the need for a vacuum pump.

Experimental results on a commercially available vacuum pump indicate that the maximum efficiency of 5.8% is achievable at approximately 50 kPa tank pressure. Below this pressure, the performance of the vacuum pump decreases.

It can also be seen from experimental results on available eductors that using the proper design for eductors through choice of motive fluid and geometry can have a significant improvement on their performance. As the experiments indicate by using the eductor which was mainly designed for using liquid (water) as motive fluid, lower absolute pressure in the tank was achieved compared to that achieved by an eductor which was designed originally for using steam as a motive fluid. Additionally, there will be an optimum motive fluid pressure for a particular eductor to get the best efficiency. For example, the examined water–gas eductor had a best performance at motive fluid pressure of 200 kPa. In this case, the maximum efficiency of 4.4% was achieved for a 30 kPa tank vacuum pressure whereas with the same eductor performing at 300 kpa motive fluid pressure, the highest efficiency of 3.1% was achieved for a tank vacuum pressure of 25 kPa. The eductor was only 1.9% efficient when it performed at motive fluid pressure of 100 kPa at almost 65 kPa air pressure.

Considering the optimum condition for the performance of the eductor, it can be concluded that the eductor is less efficient than the commercially available vacuum pump at high pressures.

5. Conclusion and future work

Considering the theoretical and experimental results, it can be concluded that two phase eductors can be utilised to remove NCGs from geothermal waters as a sustainable technology.

However, they are less efficient than the commercial vacuum pump at higher pressures, but have shown better performance than vacuum pumps at low pressures.

Therefore, the water–gas eductor is suitable for removing NCGs where a continuous water flow is available and the vacuum to be maintained is low. In addition, there is the simplicity of the eductor design with no moving parts, rugged construction, large volume capability, maintenance free operation, low cost and long life.

As the efficiency of the available methods for removing non-condensable gases from geothermal water is not very high, further research and work is needed to make them more efficient. Furthermore, for future work the efficiency of the water–gas ejector can be increased since there is large potential for improving the performance of the two phase ejector compared to that of a vacuum pump by making changes to the geometry of the ejector and optimising the design.

Acknowledgement

The authors gratefully acknowledge the financial and technical support from the GreenEarth Energy Ltd.

References

[1] Bai F, Singh R, Date A, Akbarzadeh A. Novel system for combined power generation and water desalination using renewable energy. Solar 09, the 47th ANZSES annual conference, 29 September–2 October 2009.

[2] Gunerhan GG. An upstream reboiler design for removal of noncondensable gases from geothermal steam for Kizildere geothermal power plant, Turkey. Geothermics 1999;28(6):739–57.

[3] Angulo R, Lam L, Gamiñ H, Jiménez H, Hughes E. Developments in geothermal energy in Mexico. Part six. Evaluation of a process to remove non-condensable gases from flashed geothermal steam upstream of a power plant. Journal of Heat Recovery Systems 1986;6(4):295–303.

[4] Yildirim Ozcan N, Gokcen G. Thermodynamic assessment of gas removal systems for single-flash geothermal power plants. Applied Thermal Engineering 2009;29(14–15):3246–53.

[5] Michelies EE. The influence of non-condensable gases on the Net work produced by the geothermal steam power plant. Geothermics 1982;I1(3): 163–74.

[6] Bidini G, Desideri U, Maria FD. A single flash integrated gas turbine geothermal power plant with non-condensable gas combustion. Geothermics 1999;28(1):131–50.

[7] Florescu NA. Some theoretical and experimental observations on the ultimate vacuum obtainable in vapour pumps. Vacuum 1954;4(1):30–9.

[8] Sonntag R, CB, Van Wylen G. Fundamentals of thermodynamics. sixth ed.John Wily & Sons, Inc.; 2002.

[9] Coker AK. Ejectors and mechanical vacuum systems. In: Ludwig's applied process design for chemical and petrochemical plants, fourth ed. Burlington: Gulf Professional Publishing; 2007. p. 525–73.

[10] Balamurugan S, Gaikar VG, Patwardhan AW. Effect of ejector configuration on hydrodynamic characteristics of gas–liquid ejectors. Chemical Engineering Science 2008;63(3):721–31.

[11] Elrod HG, J.. The theory of ejectors. ASME Transactions 1945:67 p. A 170.

[12] Khaghani A, Date A, Akbarzadeh A. Sustainable noncondensable gas removal from geothermal waters. Solar 2010 conference; 2010.

[13] Kandakure MT, Gaikar VG, Patwardhan AW. Hydrodynamic aspects of ejectors. Chemical Engineering Science 2005;60(22):6391–402.

[14] Ouzzane M, Aidoun Z. Model development and numerical procedure for detailed ejector analysis and design. Applied Thermal Engineering 2003;23(18): 2337–51.

[15] Zhu Y, Wenjian C, Changyun W, Yanzhong L. Numerical investigation of geometry parameters for design of high performance ejectors. Applied Thermal Engineering 2009;29(5–6):898–905.